

Chapter 6

Surface Temperature in Polishing

6.1. Introduction

As discussed in previous chapters, the dynamic friction polishing technique utilizes a thermo-chemical reaction between a PCD surface and a metal disk rotating at a high peripheral speed. The polishing mechanisms can be described as conversion of diamond into non-diamond carbon, and SiC to amorphous silicon oxide/carbide, by friction heating and contact with catalytic metals. The much softer non-diamond carbon and amorphous silicon oxide/carbide are then removed mechanically/chemically. It is clear that the chemical reactions of carbon and SiC with metals or oxygen play an important role in the material removal of PCD, and these reactions occur only at elevated temperatures.

To control and then optimize the polishing of PCD, using friction dynamics mechanisms, it is necessary to estimate the temperature during the process, find out the effective ranges of polishing speed and pressure, and then establish their relation to the material removal rate. Hence, this chapter describes the development of a model to predict the interface temperature rise of the PCD surface during polishing. Then experiments are carried out to

measure on-line subsurface temperatures for a range of polishing conditions. In addition, a method is developed to extrapolate these measured temperatures to the PCD surface. These theoretical and experimental methods give upper limit and lower limit temperatures, respectively from different points of view; and can be used to determine whether the temperature rise is high enough to stimulate chemical reactions and hence material removal during polishing.

6.2. Modelling

Greenwood-Williamson's statistical asperity model will be used to characterise the surface roughness of a PCD specimen. The result will then be used to estimate the contact area and total number of contact asperities under an applied polishing load. The heat generated will be taken as the product of the friction force and the relative sliding speed between the PCD asperities and the metal disk surface. Jaeger's moving heat source analysis will then be applied to determine the fraction of heat flux flowing into the PCD asperities in polishing and its counterpart at contact sliding and to predict the average temperature rise on the contact surface.

6.2.1 Statistical model of PCD surface roughness

During polishing, the contact between a PCD surface and the polishing disk is on a large number of asperities. Random roughness of the PCD can be characterized by a statistical asperity model [Greenwood and Williamson, 1966], which assumes: i) that all asperities are spherical at their summits and have the same radius R_a and, ii) that their heights vary

randomly: the probability that a particular asperity has a height between z and $z+dz$ above a reference plane, as illustrated in Fig.6.1 will be $\Phi(z)dz$, where $\Phi(z)$ is the height distribution of the PCD asperities. Figure 6.1 shows the schematic of the contact surfaces. The behaviour of an individual asperity during contact can be found from the Hertzian equations [Johnson, 1985]. It should be noted that the surface of the polishing metal disk is assumed to be smooth. Since the metal is much softer than PCD, the polishing forces acting through neighbouring disk asperities will influence each other, i.e., the individual contacts are not independent.

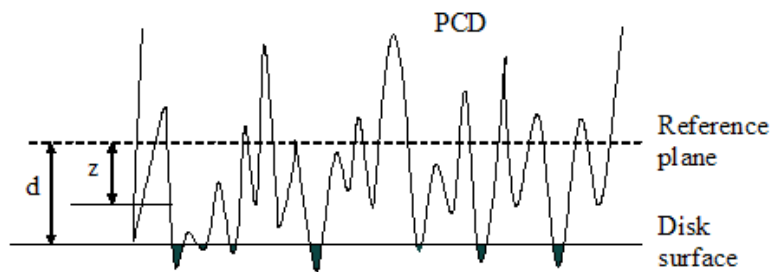


Fig.6.1 Schematic of PCD asperities-disk contact in polishing: The load is supported by the shaded asperities whose heights are originally greater than the separation d .

If the two surfaces come together until their reference planes are separated by a distance d (Fig.6.1), then contact will occur at any asperity whose height was originally greater than d [Greenwood and Williamson, 1966]. Therefore, the probability of making contact at any given asperity of height z is

$$\text{prob}(z>d) = \int_d^{\infty} \Phi(z)dz.$$

If the surface density of asperities η and the nominal contact area A are known, then the total number of asperities will be $N = \eta A$. Thus the expected number of contacts will be

$$n = \eta A \int_d^{\infty} \Phi(z) dz. \quad (6.1)$$

The expected total area of contact will be

$$A = \pi \eta A R_a \int_d^{\infty} (z - d) \Phi(z) dz. \quad (6.2)$$

The expected total load is

$$L = \frac{4}{3} \eta A E' R_a^{\frac{1}{2}} \int_d^{\infty} (z - d)^{\frac{3}{2}} \Phi(z) dz, \quad (6.3)$$

where

$$\frac{1}{E'} = \frac{1 - \nu_1^2}{E_1} + \frac{1 - \nu_2^2}{E_2}, \quad (6.4)$$

in which E and ν are Young's modulus and Poisson's ratio, and the subscripts 1 and 2 refer to the two contacting materials. The applied load L is carried by asperities in contact. The nominal pressure is $P = L/A$, and applied pressure is $P' = L/A'$, where A is the nominal area of the specimen and A' is the expected contact area. Note that $P' \gg P$ because $A' \ll A$, and that the actual contact area A' is a strong function of surface roughness, but P' is not. This suggests that P' controls polishing via the actual contact area [Yu *et al.*, 1993].

Thus, the surface characteristic function of the PCD, $\Phi(z)$, and the applied load, L , are known, then the separation of the two surfaces can be calculated by using equation (6.3).

The number of contacts n and the contact area A can then be obtained by using equations (6.1) and (6.2).

6.2.2 Temperature rise

In order to estimate the temperature rise at contact between a PCD asperity and a polishing disk, the theory of a moving heat source and the method of energy partition at contacts developed by Jaeger [Jaeger, 1942] are used. The heat generated at the contact between a PCD asperity and the polishing disk is taken as the product of the friction force acting on the asperity and the relative sliding speed V between the asperity and the disk. The average force L_1 acting on the asperity is the total load L divided by the number of contacts

$$L_1 = L/n = PA/(\eta A \int_d^{\infty} \Phi(z) dz) = P/\eta \int_d^{\infty} \Phi(z) dz. \quad (6.5)$$

Since the summits of asperities are assumed to be spherical with radius R_a , and the contact is assumed to be Hertzian, the average contact radius of the asperity is given by:

$$a = \sqrt{\frac{A'}{\pi n}} = \sqrt{\frac{R_a \int_d^{\infty} (z-d) \Phi(z) dz}{\int_d^{\infty} \Phi(z) dz}}. \quad (6.6)$$

The average heat flux at the real area of contact due to the frictional heating can therefore be expressed as [Bulsara *et al.*, 1997, Jaeger, 1942, Tian and Kennedy, 1994]

$$h = \frac{\mu L_1 V}{\pi a^2}, \quad (6.7)$$

where μ is the coefficient of friction and V is the relative sliding speed between the contacting bodies, which is determined from equations (4.1), as detailed in section 4.3.2,

Chapter 4. For an individual PCD asperity, contact between the asperity and the polishing disk is Hertzian, tangential friction force has a parabolic distribution, and the tangential frictional stress is given by [Johnson, 1985]

$$q(x) = \frac{3\mu L_1}{2\pi a^3} (a^2 - x^2)^{1/2}.$$

Thus the heat flux generated due to the tangential friction force also has a parabolic distribution over the contact area.

The frictional heating of a PCD asperity can be modelled as a heat source moving over the surface of a semi-infinite polishing disk with speed V , as the disk and PCD specimen are much bigger than the asperities. An analytical formulation for the temperature under a square or a band heat source moving over the surface of a semi-infinite solid was presented by Jaeger [Jaeger, 1942]. Later in 1994, Tian and Kennedy [Tian and Kennedy, 1994] derived an approximate solution for the interface temperature rise under a moving circular heat source for the entire range of Peclet numbers P_e which, representing the scale of the velocities in a moving heat source, is defined as [Bulsara *et al.*, 1997, Tian and Kennedy, 1994]

$$P_e = \frac{Va}{2\chi} = \frac{Va\rho C}{2K},$$

where $\chi=K/(\rho C)$ is thermal diffusivity, K is thermal conductivity, C is specific heat, and ρ is the density of material exposed to the heat source. In this paper, P_e refers to the Peclet number of the polishing disk material.

The frictional heating of a PCD asperity can be modeled as a heat source moving over the surface of a semi-infinite polishing disk with speed V . According to Tian and Kennedy [Tian and Kennedy, 1994], the average, steady-state surface temperature rise T_r over the area of contact due to a circular parabolic heat source h moving over a homogeneous semi-infinite solid with speed V is

$$T_r = \frac{1.464ah}{K \sqrt{\pi(0.874 + P_e)}}. \quad (6.8)$$

For a stationary parabolic circular heat source h , the temperature rise is

$$T_r = \frac{9Q}{32RK} = \frac{9\pi ah}{32K}. \quad (6.9)$$

According to Jaeger [Jaeger, 1942], when a steady state has been attained, it can be assumed that a fraction α of the heat h per unit time per unit area generated over the area of contact passes on to the polishing disk and the remaining fraction $(1-\alpha)$ to the PCD asperity. The fraction α can therefore be determined by the condition that at the contact interface, the average temperature on the disk surface equals that on the PCD surface, if there is no heat loss to the surroundings. Equating these temperature rises, given by equations (6.8) and (6.9) for the asperity and the disk surfaces over the circularly shaped area of contact gives rise to

$$\frac{1.464ah\alpha}{K_d \sqrt{\pi(0.874 + P_e)}} = \frac{9\pi ah(1-\alpha)}{32K_p}. \quad (6.10)$$

The subscripts d and p refer to the disk and PCD asperity, respectively. From Eq. (6.10), the heat flux fraction α going into the polishing disk is

$$\alpha = \frac{9\pi K_d \sqrt{\pi(0.874 + P_e)}}{46.848K_p + 9\pi K_d \sqrt{\pi(0.874 + P_e)}}. \quad (6.11)$$

The contact temperature rise at the sliding interface is therefore:

$$T_r = \frac{13.176\pi ah}{46.848K_p + 9\pi K_d \sqrt{\pi(0.874 + P_e)}}. \quad (6.12)$$

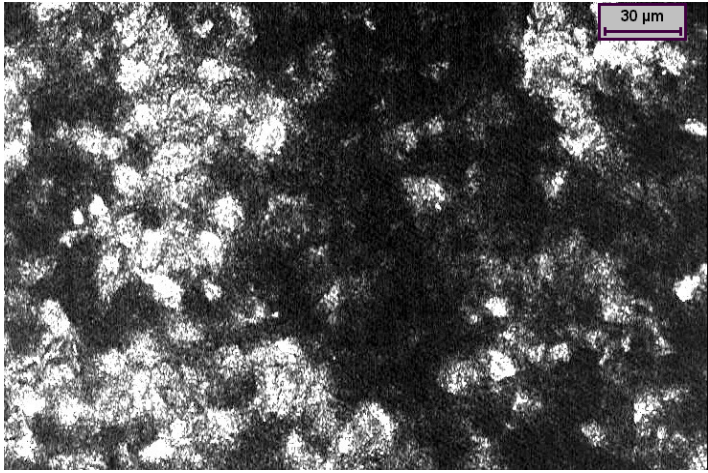
The above analysis gives an upper bound estimation because the heat loss into the surrounding has been neglected. Since the model calculates the average temperature rise on the asperity over the contact area, hot spots (flash temperatures, which could be significantly higher in polishing) cannot be estimated.

In the model developed above, when the applied load and the surface characteristics (including the function $\Phi(z)$, radius of asperity R_a and the asperity density η) are known, the number of contacts n and the contact area A' can be calculated by using equations (6.1), (6.2) and (6.3). Then from equation (6.7), the average heat flux h can be obtained after the average force L_l and the contact radius of asperity a are determined from equations (6.5) and (6.6), respectively. Finally the average contact temperature rise can be calculated from equation (6.12).

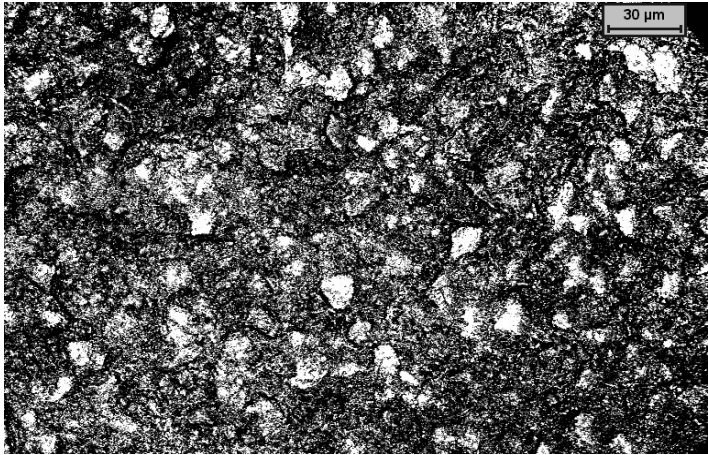
6.3. Experimental Measurement of Surface Topography

In order to calculate the expected number of contacts and the total area of contact, the topographic parameters should be measured. These parameters include average radius of asperity summits, the surface density of asperities and the spread of asperity heights. For

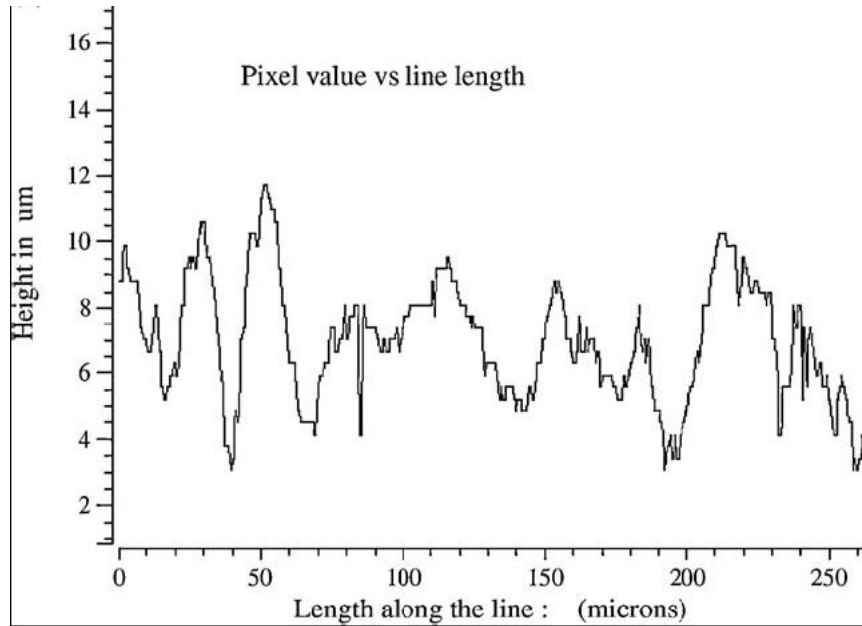
this purpose, the confocal microscope technique used by Zhang and Zarudi [Zhang and Zarudi, 1999] was employed. With the confocal microscope, a series of pictures in focus on different layers can be obtained, Fig.6.2 (a). These pictures can be compiled to an extended focus image, Fig.6.2 (b). Then on a selected line, a surface roughness diagram can be acquired as shown in Fig.6.2 (c) to generate the surface roughness data.



(a) One of the series pictures



(b) The extended focus picture



(c) Surface roughness diagram

Fig.6.2 The surface topography of a PCD specimen before polishing, generated by confocal microscopy

By using the microscopy analysis software LEICA QWin, these extended focus images were analysed. From the results of asperity field analysis, the area of asperity, the number of asperities (count), the total area of analysed frame and the ratio of count to frame area were obtained. For the PCD compact used in the present experiment, the average asperity density η was found to be 2.2×10^5 asperities/mm². From an analysis of the asperity features, it was found that the mean equivalent diameter of asperities was 0.90 μm , hence the average radius of the asperities was calculated to be 0.45 μm .

By using an Excel statistical data analysis tool: *Histogram and Descriptive Statistics*, it was found that the asperity heights on the surface would approximately obey a Gaussian

distribution, $\Phi(z) = \frac{1}{\sigma\sqrt{2\pi}} e^{-\frac{z^2}{2\sigma^2}}$, with an average height of 0 (which is the asperity height reading from the mean plane) and a standard deviation of 2.0 μm . The standard deviation σ of the distribution is identical to the root mean square roughness value of the surface [Xie and Williams, 1996]. In the present work, the maximum asperity height was 5.0 μm and hence this value was used instead of infinity for the integrations in equations (6.1), (6.2), (6.3), (6.5) and (6.6).

It should be noted that the surface characteristics R_a and N of a randomly rough surface are not unique but depend on the resolution and the scan length of the roughness-measuring instrument [Xie and Williams, 1996]. Only the standard deviation σ can be approximately taken as scale-independent. Thus only the asperities which have a roughness of the same order of magnitude as that of the overall σ value can be counted.

6.4. Predicted Results and Discussion

The contact interface temperature rise for the polishing of PCD using a metal disk has been estimated using the temperature model derived above. Table 6.1 gives the material properties of the PCD and the steel used for the calculations. It must be pointed out that the properties of PCD are strongly dependent on composition, particle size, and processing conditions. For example, the thermal conductivity of a PCD can range from 250 to 920 W/m.K [Field, 1992, Jahanmir *et al.*, 1998, Klimenko *et al.*, 1996, Pope *et al.*, 1975, Wilks and Wilks, 1994], and some PCD films made by synthetic diamond can have a thermal

conductivity up to 1200-1800 W/m.K [Klimenko *et al.*, 1996]. For the present PCD, some of the data such as thermal conductivity, the Poisson's ratio and density were measured experimentally. The coefficient of friction between the disk and PCD asperity was taken to be 0.15 based on the measurement by Iwai *et al.* [Iwai *et al.*, 2001]¹. A MATLAB program was developed for calculating the temperature rise.

Table 6.1 Properties of PCD and catalytic steel

	Catalytic steel	PCD
Young's modulus E	200 GPa	900 GPa
Poisson's ratio ν	0.28	0.10
Thermal conductivity K	16.3 W/m.K	300 W/m.K
Density ρ	8000 kg/m ³	3520 kg/m ³
Specific heat C	500 J/kg.K	470 J/kg.K

Figures 6.3 and 6.4 show the variations of the calculated average contact temperature rise with the sliding speed and nominal applied pressure. According to these figures, the higher values of P and V correspond to a higher heat flux h and higher temperature rise T_r . The temperature rise T_r is seen to increase with increasing P and V . The dependence of T_r on V appears to be linear for a fixed nominal pressure (Fig.6.3). However, for a fixed sliding speed V , the relation between T_r and P seems to follow a power law (Fig.6.4). It can also be seen that speed has a greater influence on temperature rise T_r (indicted by a higher slope) than pressure.

¹ The coefficient of dynamic friction was measured to be from 0.13 to 0.2 at pressures 17 and 27 MPa with a mean value of about 0.15.

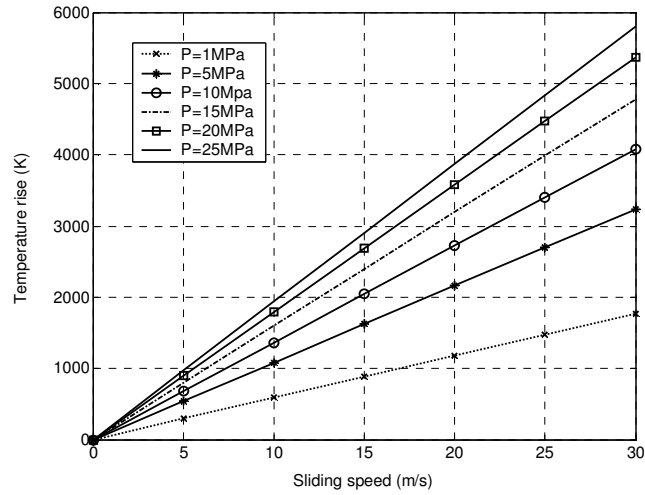


Fig.6.3 Variation of calculated average temperature rise with sliding speed at different nominal pressures

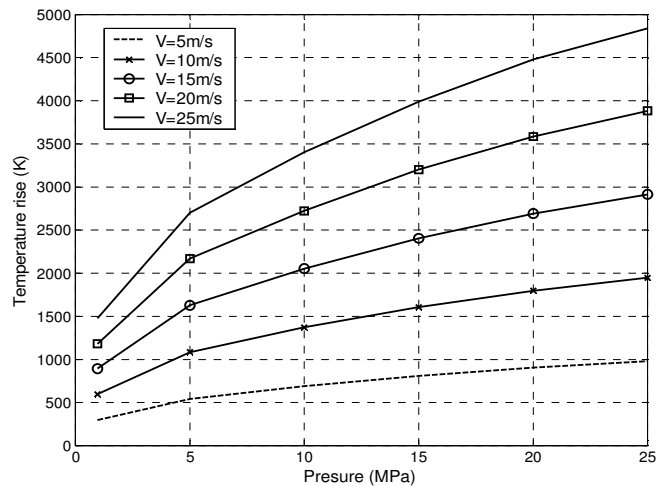


Fig.6.4 Variation of calculated average temperature rise with nominal pressure at different sliding speeds

From equation (6.12), it can be seen that the temperature rise is dependent not only on the sliding parameters (V and P), but also on surface characteristics and properties of the two sliding materials, especially their thermal conductivities. Thus, we have also predicted a

temperature rise for varying values of the PCD's thermal conductivity. The other data used for the calculation are given in Table 6.1. These predicted results are given in Fig.6.5. As expected, higher values of PCD's thermal conductivity result in lower values of temperature rise at the interface. For example, when the thermal conductivity of PCD increases twice, the temperature rise drops to 50%.

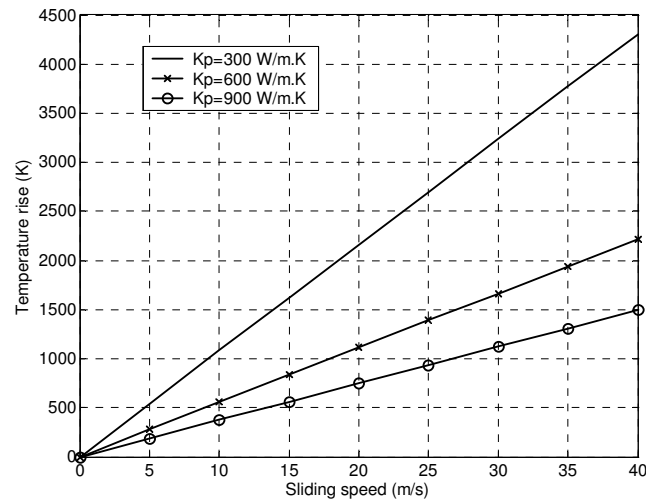


Fig.6.5 Variation of temperature rise with sliding speed at different thermal conductivity values of PCD at pressure 5 MPa

The surface roughness of PCD also affects the temperature rise. Figure 6.6 compares the temperature rise for different values of standard deviation $\sigma = 1, 2$ and $4 \mu\text{m}$. In the calculations, the maximum height of the asperity was selected to be 2.5σ , which is the appropriate value for the PCD used in the present work. The results given in Fig.6.6 show that a higher surface roughness of PCD results in a higher temperature rise, because there are fewer asperities in contact under the same nominal pressure and hence a higher average load on contact asperities. This means that when polishing proceeds, the polishing speed or pressure should be increased if one needs to maintain the same temperature rise for the sake

of efficient polishing (neglecting the heat accumulation), because the surface roughness of a PCD specimen decreases during polishing.

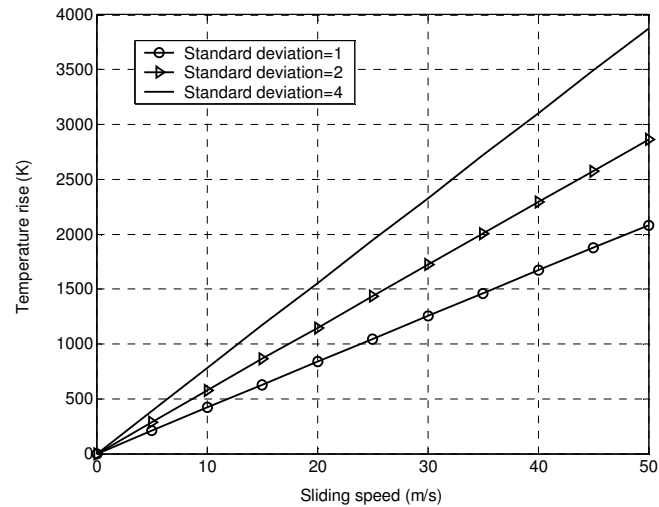


Fig.6.6 Variation of temperature rise with sliding speed at different surface roughness at pressure 5 MPa

In the above calculations, it is assumed that the material properties such as Young's modulus E and thermal conductivity K do not vary with temperature. While the details of the temperature-dependence of E and K for PCD could not be found, the information available seems to indicate that for both the catalytic steel and PCD, E decreases whereas K increases with the increase in temperature [Lord and Orkney, 2000, Lytton *et al.*, 1964, Pope *et al.*, 1975]. A decrease in E will cause an increase in pressure and hence an increase in the calculated temperature. On the other hand, an increase in K will lead to a decrease in the calculated temperature. Therefore, the variation of E and K with temperature may not have a large influence on the calculated temperature rise, due to the balancing of their opposing effects.

6.5 Comparison with Results from the Literature

A direct measurement of temperature rise at the polishing interface is almost impossible at present, so is a direct quantitative comparison of the theoretical prediction with experimental ones. However, the following experimental observations seem to support the theoretical estimations.

In one of the preliminary tests, the PCD surface topography was measured as described in section 6.3. The polishing parameters were: sliding speed approximately 15 m/s and pressure 5 MPa. During polishing, the steel disk turned red, and lots of sparkles were observed. It was noted that due to the frictional heat, the steel disk surface melted and adhered to the PCD surface. Obviously, the temperature at the interface was raised above the melting point of steel (1421°C). From our predicted results (shown in Fig.6.3), the temperature rise for the above sliding speed and pressure is 1623°C. It is noteworthy that the interface temperature may not increase beyond the melting point of steel. In addition, as highlighted in section 6.2.2, the developed model tends to overestimate the interface temperature, as it does not account for the heat loss to the surrounding environment. Therefore, the estimated temperature rise seems reasonable.

Iwai *et al.* [Iwai *et al.*, 2001] reported that, at pressure 27MPa and sliding speeds above 10.5 m/s, the polishing efficiency increased linearly with the increase in speed. However, at lower sliding speeds (i.e. those below 10.5 m/s), PCD could not be polished. The reason is that at low speeds, the temperature rise due to the dynamic friction is not high enough for

the fast chemical reaction of diamond to occur. In the present work, an attempt was made to predict the interface temperature using the described predictive method for the conditions used in Iwai *et al.* [2001]. The surface roughness and properties of PCD used in the above study which were kindly provided by Iwai [2005] are given in Table 6.2. The properties of steel used in the calculations are the same as those given in Table 6.1. The average asperity radius R_a and asperity density N of PCD were assumed to be the same as those given in section 6.3. For the conditions used by Iwai *et al.*, the predicted variation in temperature rise with sliding speed is shown in Fig.6.7. It can be seen that, at sliding speed 10.5 m/s, the estimated temperature rise is approximately 650 °C. This value may be the minimum temperature rise required for the fast chemical reaction to occur at the PCD interface.

Table 6.2 Surface roughness and properties of the PCD used in [Iwai, 2005, Iwai *et al.*, 2001]

Young's modulus E	776 GPa
Poisson's ratio ν^*	0.10
Thermal conductivity K	560 W/m.K
Density ρ	4120 kg/m ³
Surface roughness standard deviation	0.63 μm

*Since ν is not given in [Iwai, 2005, Iwai *et al.*, 2001] , it is assumed to be the same as that of PCD used in the present study.

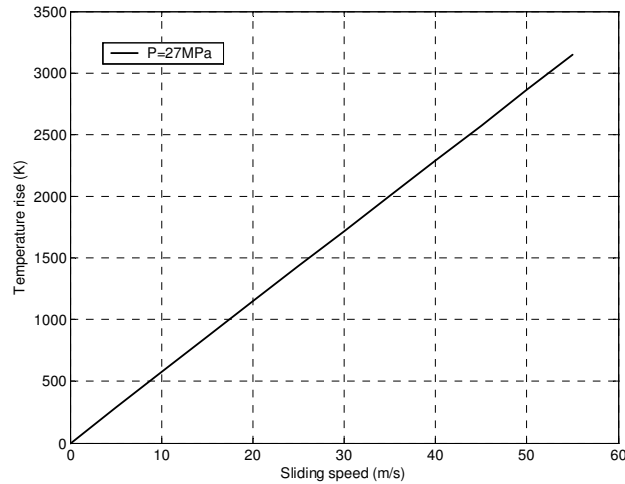


Fig.6.7 Variation of temperature rise with sliding speed for the conditions used in [Iwai, 2005, Iwai *et al.*, 2001]

6.6 On-line Temperature Measurement

At present, it is difficult to measure the interface temperature during PCD polishing. Though some surface thermocouples have been used to measure temperature [Kennedy *et al.*, 1997], fitting them in a rotating polishing disc would be difficult and the thermocouple could only contact the PCD surface once per revolution of the disc. Moreover, fitting the thermocouple in the PCD surface might affect the heat flow pattern significantly, and the measured temperature would be likely to be the interface between disk and thermocouple instead of PCD. Thus an attempt was made to measure the PCD subsurface temperature, and then extrapolate these temperatures to the polishing surface.

6.6.1 Experimental set up

The PCD specimens used were thermally stable diamond compacts, containing 70-75% diamond particles of 25 μm grain size (the balance is SiC and Si). Properties of the PCD are shown in Table 6.1. The surface roughness and topography before polishing were as discussed in Section 6.3. The dimensions of the PCD specimen used for the temperature measurement are shown in Fig. 6.8.

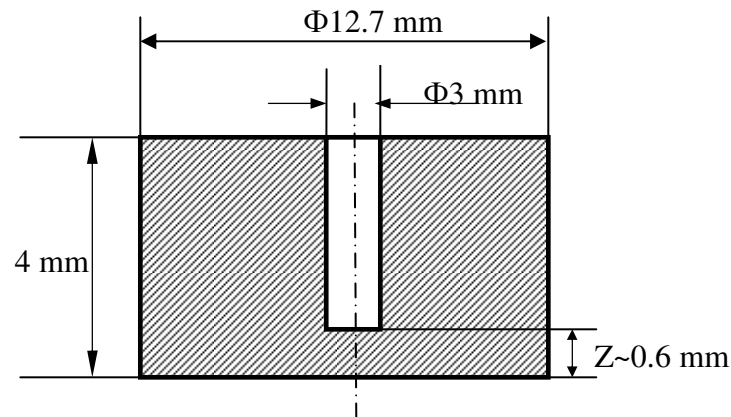


Fig. 6.8 Dimensions of PCD specimen used for the temperature measurement

The PCD's subsurface temperature was measured on-line while polishing it on the in-house built diamond polishing machine described in Chapter 4. K type thermocouple (Cr-Al) wires used were twisted and clamped together to make a hot junction. Figure 6.9 depicts the configurations of the thermocouple in the PCD specimen for temperature measurement. The thermocouple was set in a hole at the centre of the PCD specimen, touching the bottom of the hole, which was around 0.6 mm from the polishing surface. Then the hole was filled with insulator alumina (Al_2O_3) powder and high temperature superglue on top of the powder, for clamping and insulating the thermocouple.

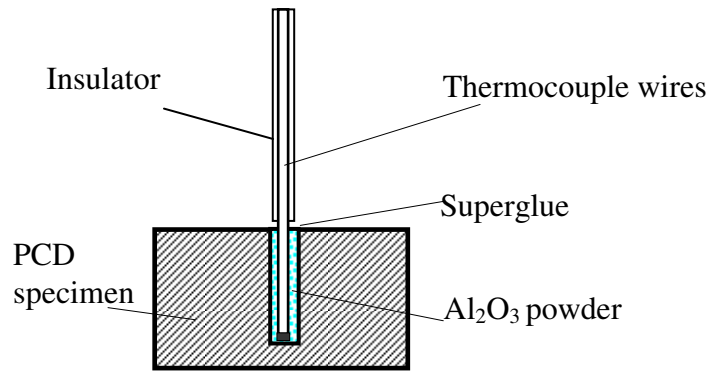


Fig. 6.9 Configuration of thermocouple in the PCD specimen

After the PCD specimen and thermocouple were installed in the polishing machine, as shown in Fig. 6.10, the thermocouple was connected to a data taker (DT800) and a personal computer with data logger software (DeLogger). After the connection, it was necessary to set up the logger and make/select a proper program and parameters for thermocouple measurement in the computer. After installation and programming, the system was calibrated with boiling water to ensure the good contact of thermocouple with the measuring point, before every on-line measurement of the polishing temperature. During measurement, the measured temperature along with polishing time was displayed on the computer screen.

A number of experiments with different combinations of pressure, speed and surface roughness were carried out. During on-line temperature measurement, the specimen holder motor was fixed and only the main disk motor was rotating. The main disk rotated first, and polishing was conducted by pressing the PCD specimen at a predetermined pressure on to the rotating metal disk in dry atmosphere. When polishing finished, the specimen was

lifted up quickly and the main motor stopped. Polishing parameters were selected based on the optimized polishing conditions to produced crack-free polishing surfaces (as detailed in Chapter 8). The sliding speed between the specimen and the metal disk varied from 12 to 25 m/s; the polishing pressure used was 2.9, 3.1, 3.8 and 5.0 MPa respectively; and polishing time was 2 minutes.

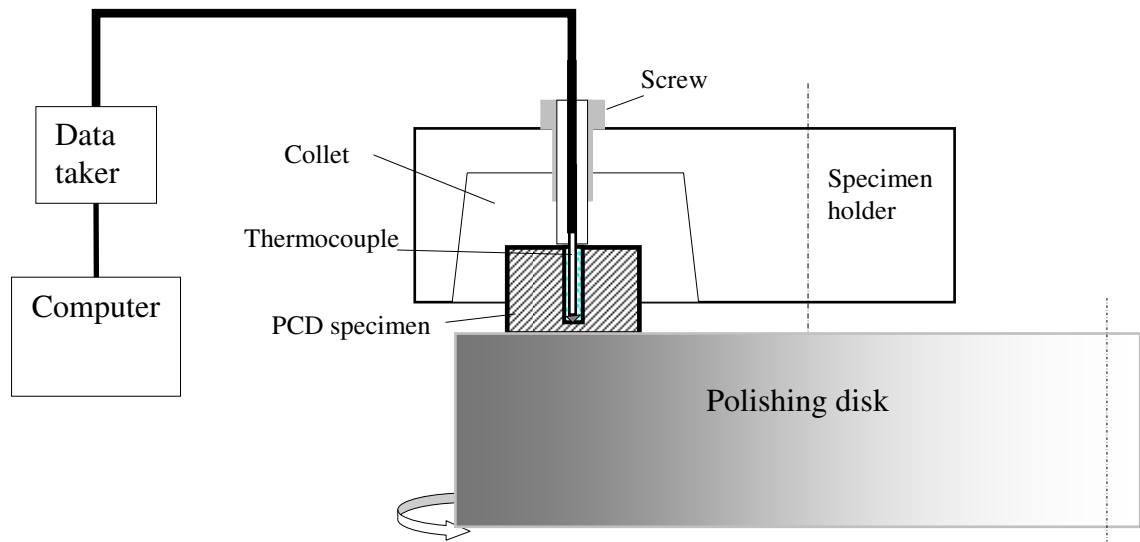


Fig. 6.10 Schematic illustration of the set up for temperature measurement

6.6.2 Measured results and discussion

Temperature variation with time was recorded with data logger software DeLogger. Figure 6.11 shows a typical measured temperature result when the experiment was carried out at polishing pressure 2.9 MPa, speed 22 m/s and polishing time two minutes. From the results (Fig.6.11), it can be seen that the temperature increases fast as the polishing starts; it rises to approximately 500 °C in less than 20 seconds, then reaches an equilibrium state and remains in the range of 430-600 °C until polishing finishes. After lifting the specimen from the polishing disk, the temperature drops quickly to near room temperature in one or two

minutes, due to the high thermal conductivity of the PCD. It is noticed that at higher polishing speeds and pressures, the temperature increases faster.

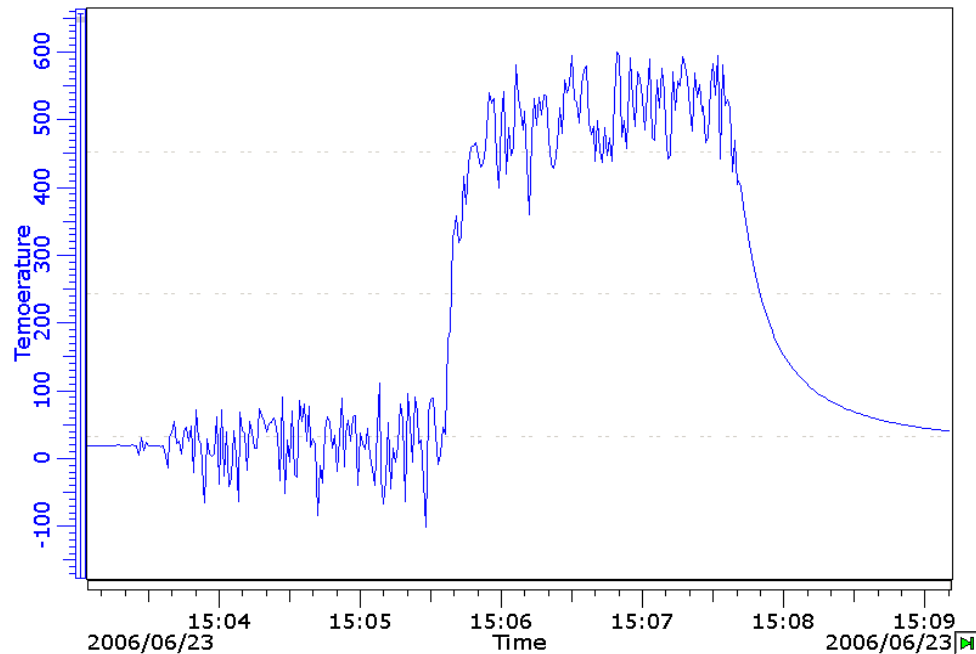


Fig. 6.11 Measured temperature results at pressure 2.9 MPa, speed 22 m/s and polishing time two minutes

The temperature fluctuations in the range result from the high speed rotating motor which causes external noise to the temperature signal. Although efforts had been made to shield the motor and the thermocouple wires, such as covering them, the noise could only be reduced, but could not be eliminated when the motor was rotating in the polishing. The noise could be neglected before the motor began rotating (as shown in Fig.6.11). At a higher sliding speed, the temperature signal noise was stronger; the displayed temperature fluctuated more frequently at higher amplitude.

It is also noted that at the same sliding speed and nominal pressure but using a PCD specimen with different surface roughness, the measured mean temperature only varied slightly between 460-470 °C, as shown in Table 6.3. This probably confirms the findings of Gecim and Winer (1984 and 1986) that regardless of the number of heat sources and their distribution on the surface, the bulk temperature rise remained the same if the cumulative heat input was fixed [Gecim and Winer, 1984, 1986, Tian and Kennedy, 1993]. Surface roughness affects the surface temperature but does not affect the bulk temperature significantly.

Table 6.3 The measured mean temperatures at different surface conditions (other polishing parameters held constant)

	1. Adhered surface	2. Cleaned surface	3. EDM surface
Roughness Ra(um)	0.2~ 0.6	0.1~ 0.4	1.6
Distance from interface (mm)	0.67	0.65	0.65
Load (kg)	48.5	48.5	48.5
Pressure (MPa)	3.8	3.8	3.8
Speed (m/min)	18	18	18
Time (min)	2	2	2
Temperature (°C)	460	460	470

Additional results from temperature measurement at different conditions are shown in the first four rows of Table 6.4. From these data, it can be seen that at an identical speed, higher pressure results in higher mean temperature. However, at a given pressure, the temperature does not increase proportionally with speed. For example, at pressure 3.1 MPa, the

measured temperature increases from 475 °C to 545 °C, when polishing speed increases from 12 m/s to 16 m/s, while the temperature only increases 5 and 15 °C when the speed increases from 16 to 20 and 25, respectively. This may be because, at higher speeds the convective cooling effect of the PCD specimen is stronger, and more heat is lost to the environment. However, convective effects would not affect the interface temperature much. The measured temperature needs to be extrapolated to the surface, at which the temperatures stimulate the chemical reaction.

Table 6.4 Measured mean temperatures and predicted temperatures under different polishing parameters

Pressure (MPa)	5	5	2.9	2.9	3.1	3.1	3.1	3.1
Speed (m/s)	14	22	14	22	12	16	20	25
Distance from PCD surface to bottom of hole (mm)	0.51	0.53	0.54	0.55	0.51	0.52	0.54	0.56
Measured mean T_z (°C)	610	620	465	515	475	545	550	560
Extrapolated to surface T_s (°C)	953	979	738	821	742	856	873	897
Predicted interface temperature rise T_r (°C)	1515	2377	1237	1942	1088	1450	1811	2262

6.6.3 Extrapolation of the measured temperature to the surface

The measured temperatures are extrapolated to the surface temperatures by using the traditional model of a steady temperature in a semi-infinite cylinder due to heat supply over a circular area [Carslaw and Jaeger, 1959]. The calculation is based on the assumptions that heat is supplied over the circular area $0 \leq r < R_p$, at the surface $Z=0$, and the circular surface

is maintained at temperature T_s , with no flow of heat over $r > R_p$. The temperature T_z at any point $Z > 0$, over $0 < r < R_p$ is [Carslaw and Jaeger, 1959]:

$$T_z = \frac{2T_s}{\pi} \int_0^{\infty} e^{-\lambda Z} J_0(\lambda r) \sin \lambda R_p \frac{d\lambda}{\lambda} = \frac{2T_s}{\pi} \sin^{-1} \left[\frac{2R_p}{\sqrt{(r-R_p)^2 + Z^2} + \sqrt{(r+R_p)^2 + Z^2}} \right] \quad (6.13)$$

where Z is the distance from the polishing surface in the PCD specimen (Fig.6.7), and R_p is the PCD specimen radius. Since the model assumes no flow of heat over $r > R_p$, we consider only part of the specimen with a small cylindrical column with the hole diameter 3 mm and the Z distance from the specimen polishing surface to the bottom of the hole, as shown in Fig.6.7.

In the present application, the temperature T_z at the bottom surface of the hole, which is Z distance from the polishing surface, is measured. Therefore the surface temperature T_s is:

$$T_s = \frac{\pi T_z}{2} / \sin^{-1} \left[\frac{2R_p}{\sqrt{(r-R_p)^2 + Z^2} + \sqrt{(r+R_p)^2 + Z^2}} \right] \quad (6.14)$$

Here, $R_p = 1.5$ mm, $r = 1.5$ mm were substituted in the calculation, since only the small cylinder of 3 mm diameter is considered. The calculated surface temperature results from the measured temperatures at different conditions are shown in the fifth row of Table 6.4.

6.7 Discussion

It should be noted that the measured temperature extrapolated to the surface is not the interface temperature at asperity contact but the average temperature over the whole PCD

surface, because it is assumed that the whole circular surface was maintained at temperature T_s . The interface temperature rises between PCD asperity and polishing disk under these polishing conditions are calculated as in section 6.4, and the results are shown in the sixth row of Table 6.4. For clarity, extrapolated temperature T_s from the experimental measurement and the predicted interface temperature rise T_r plotted against sliding speed at polishing pressure 3.1 MPa are shown in Fig. 6.12.

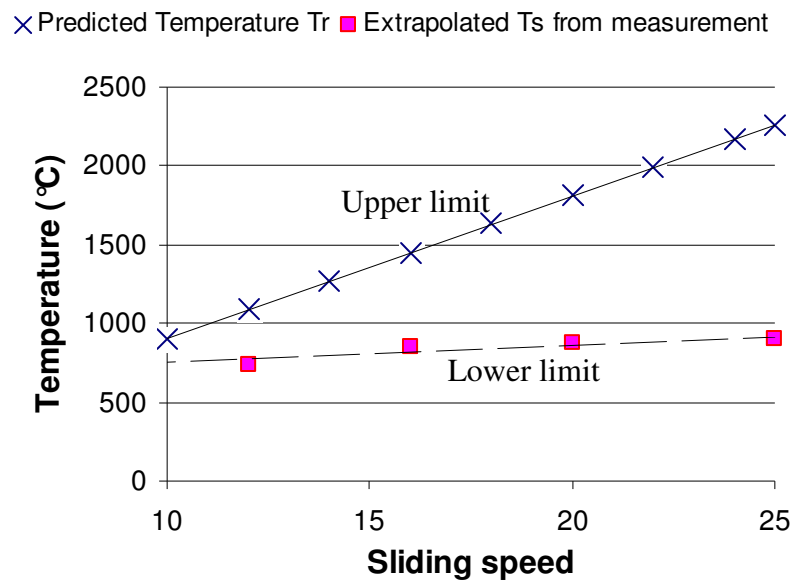


Fig. 6.12 Variation of extrapolated temperature T_s and predicted interface temperature rise T_r with polishing speed at polishing pressure 3.1MPa

As can be seen from Table 6.4 and Fig. 6.12, at an identical sliding speed and pressure, the predicted temperature rise at the asperity contact interface is significantly higher than the extrapolated temperatures from experimental measurement, because the load only acts on a small area of asperity contact. The interface temperature rise due to dissipation of frictional heat at the contacting asperity peaks can be of a higher magnitude, but will be limited to a short duration ant to the interface region [Kalin, 2004]. A significant temperature drop can

exist at the contact interface, because the real contact area is much smaller than the nominal contact area [Attia and Ko, 1986, Guha and Roy Chowdhuri, 1996, Tian and Kennedy, 1993].

In addition, as mentioned in section 6.2.2, as it is assumed that there is no heat loss into the surrounding, the above theoretical calculated temperatures are the upper bound estimations. However, during temperature measurement, especially at high speed polishing, a considerable proportion of heat is lost to the environment due to the convection cooling, which has less effect on the interface temperature. Therefore, the extrapolated temperatures from measurement are the lower limit of surface temperatures during polishing.

6.8 Conclusions

A theoretical model was developed to estimate temperature rise at the interface of the polishing disk and PCD asperities. The effects of PCD surface roughness, material properties, polishing speed and polishing pressure on the surface temperature rise were studied using the developed model. On-line temperature measurements were carried out to determine subsurface temperatures for a range of polishing conditions. A method was also developed to extrapolate these measured temperatures to the PCD surface. The predicted interface temperature gives an upper limit and the extrapolated temperature from measurement gives a lower limit of the polishing temperature.